

ARTICLE OPEN



The combination of hydroxychloroquine and 2-deoxyglucose enhances apoptosis in breast cancer cells by blocking protective autophagy and sustaining endoplasmic reticulum stress

Ning Zhou^{1,5}, Qingyun Liu^{2,5}, Xiao Wang¹, Lixin He¹, Tao Zhang³, Han Zhou¹, Xinying Zhu^{1,4}, Tianhong Zhou¹, Ganzhen Deng¹ and Changwei Qiu¹✉

© The Author(s) 2022

2-Deoxyglucose (2-DG) can be used in antitumour research by inhibiting glycolysis and promoting the endoplasmic reticulum stress (ERS) pathway, but its clinical application is restricted due to dose-limiting side effects and survival chance for cancer cells by protective autophagy. Therefore, our research explored whether the combination of hydroxychloroquine (HCQ), an FDA-approved autophagy inhibiting drug, and 2-DG is a promising therapeutic strategy. Here, we report that HCQ combined with 2-DG can further inhibit the viability and migration and induce apoptosis of breast tumour cells compared with other individual drugs. The combination of 2-DG and HCQ can significantly reduce transplanted tumour size and tumour cell metastasis of the lung and liver in vivo. At the cellular level, HCQ suppressed autolysosome formation and terminated the autophagy process induced by 2-DG-mediated ERS, resulting in the continuous accumulation of misfolded proteins in the endoplasmic reticulum, which generated sustained ERS through the PERK-eIF2 α -ATF-4-CHOP axis and triggered the transformation from a survival process to cell death. Our research reinforced the research interest of metabolic disruptors in triple-negative breast cancer and emphasized the potential of the combination of 2-DG and HCQ as an anticancerous treatment.

Cell Death Discovery (2022)8:286; <https://doi.org/10.1038/s41420-022-01074-6>

INTRODUCTION

Breast cancer is one of the most commonly diagnosed tumours in women [1]. Despite the clinical application of new techniques such as early detection, imaging and targeted therapy, a large number of women die each year of breast cancer progression [2]. Canine breast tumours (CMTs) are also one of the high incidence types of tumours in unneutered dogs [3]. CMTs are one of the best animal models for studying human tumours because they share similar physiological, genetic, and epidemiological characteristics [4]. However, the currently used chemotherapy drugs are limited due to their strong cytotoxic side effects and drug resistance [5, 6]. Thus, safe and effective novel therapeutic strategies are urgently needed.

Cancer cells are more likely to obtain energy from glucose by glycolysis than normal cells, which produce ATP through oxidative phosphorylation [7]. Therefore, the suppression of glycolysis is considered an effective potential therapeutic strategy for breast tumours [8].

2-Deoxyglucose (2-DG) is a glucose analogue, and it can bind to glucose transporters, which are key proteins for glucose

absorption, to competitively inhibit glucose absorption and further inhibit glycolysis [9, 10]. In addition, 2-DG-GDP is a downstream product of 2-DG metabolism, which can interfere with N-linked glycosylation due to its similarity to mannose-GDP in structure [11]. Therefore, 2-DG can also induce the continuous accumulation of unfolded/misfolded proteins in the endoplasmic reticulum (ER), which could cause endoplasmic reticulum stress (ERS) and subsequent death [12, 13]. On the other hand, ERS activates protective autophagy and mediates the elimination of defective proteins and organelles, which may be the reason why 2-DG monotherapy has yielded few positive results [14, 15].

Hydroxychloroquine (HCQ) is widely used in the treatment of clinical diseases, including rheumatology and infectious diseases [16, 17]. Moreover, recent research evidence shows the positive role of HCQ in oncology research because it can inhibit autophagy by deacidifying lysosomes [18, 19].

In this study, we show that the combined treatment of HCQ and 2-DG has a synergistic effect on inhibiting the viability of 4T1 cells (mouse origin) and CMT-7364 cells (canine origin) under the mechanism of autophagy inhibition and sustained ERS.

¹Department of Clinical Veterinary Medicine, College of Veterinary Medicine, Huazhong Agricultural University, Wuhan, Hubei 430070, China. ²State Key Laboratory of Agricultural Microbiology, College of Veterinary Medicine, Huazhong Agricultural University, Wuhan, Hubei 430070, China. ³Department of Clinical Veterinary Medicine, College of Animal Science and Technology, Anhui Agricultural University, Hefei 230036, China. ⁴Department of Animal Science and Technology, Shanghai Agriculture and Forestry Vocational College, Shanghai 201699, China. ⁵These authors contributed equally: Ning Zhou, Qingyun Liu. ✉email: sdqiu2001@mail.hzau.edu.cn

Received: 5 March 2022 Revised: 12 May 2022 Accepted: 27 May 2022

Published online: 11 June 2022

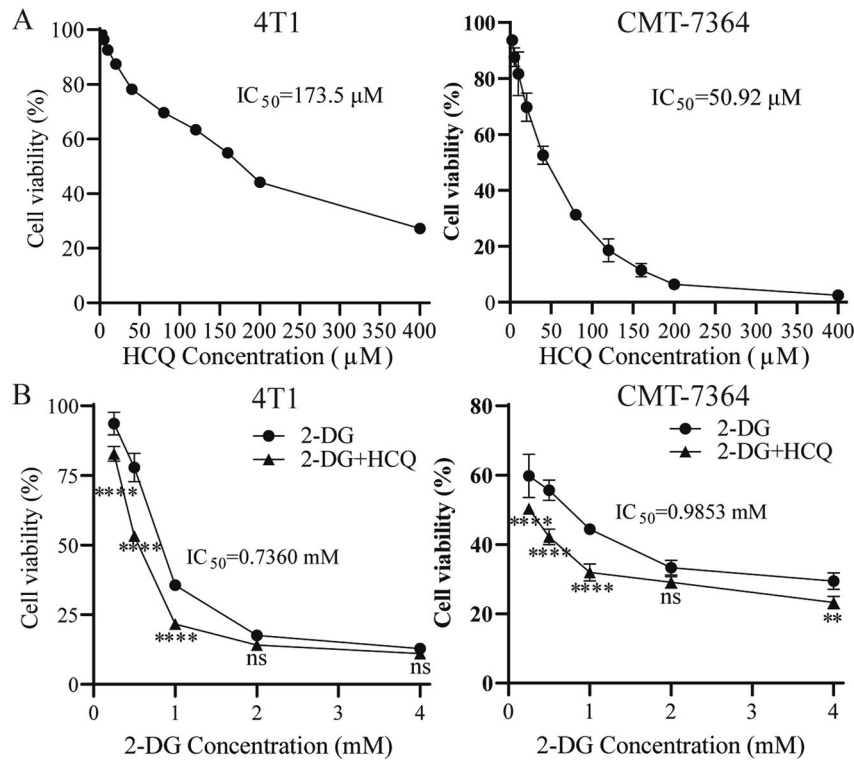


Fig. 1 HCQ and 2-DG inhibit breast cancer cell viability. **A, B** The 24 h IC₅₀ values of HCQ and 2-DG were calculated in 4T1 and CMT-7364 cells. Cell viability was determined via the Cell Counting Kit-8. The combination of 2-DG and HCQ had a stronger cytotoxic effect on cell viability than 2-DG alone. $n = 5$ for each group. Data are presented as the means \pm SD of three independent experiments. ** $p < 0.01$, **** $p < 0.0001$, ns = not significant ($p \geq 0.05$).

RESULTS

HCQ and 2-DG display cytotoxicity on breast cancer cells

As previously reported, HCQ and 2-DG are cytotoxic to a variety of cancer cells [12, 19]. To explore the mode of action of drugs in different species of breast tumours more comprehensively, we chose CMT-7364 and 4T1 cells, which are all usually applied models of human breast tumours. Cells treated with increasing concentrations of HCQ or 2-DG showed a dose-dependent decrease in viability (Fig. 1A, B). The IC₅₀ values of CMT-7364 and 4T1 cells treated with HCQ were both $>50 \mu\text{M}$. Based on these results and previous reports, we chose $10 \mu\text{M}$ HCQ for further studies. In contrast to 2-DG alone, $10 \mu\text{M}$ HCQ combined with different concentrations of 2-DG increased cytotoxicity (Fig. 1B). The IC₅₀ of 2-DG in CMT-7364 and 4T1 cells was approximately equal at 0.9853 and 0.7360 mM, respectively. Based on these findings, 1 mM 2-DG was used for further experiments.

HCQ combined with 2-DG exerts a higher anticancer activity in vitro

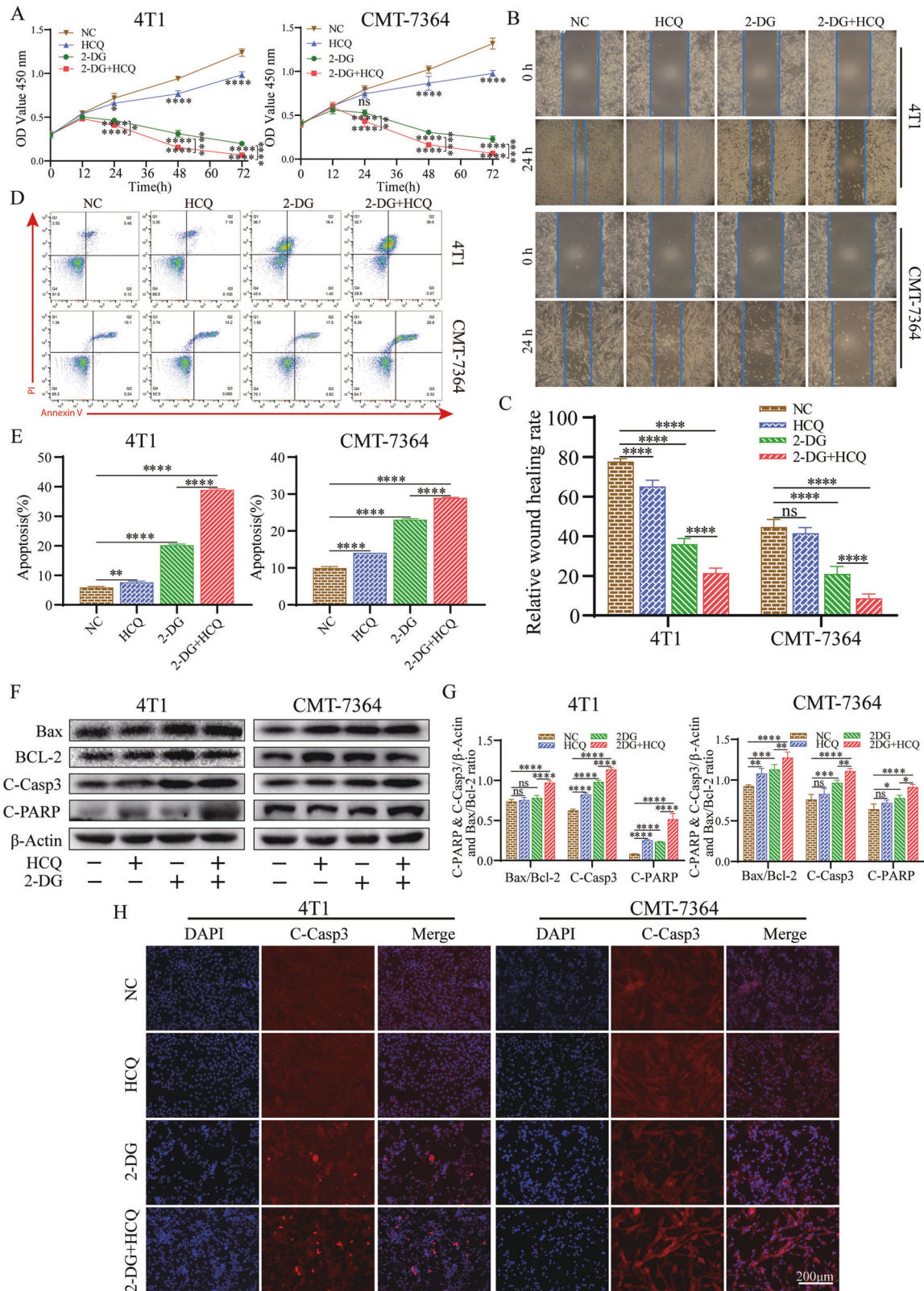
2-DG has been shown to inhibit cell proliferation and induce cell apoptosis in breast neoplasms but usually needs to be combined with other drugs to obtain better results [19, 20]. Compared with the NC group, treating with different concentrations of 2-DG all significantly increased the expression of apoptotic proteins in CMT-7364 cells (Figure S1). While, there was no difference in these protein expression levels between the different concentration groups (Figure S1), suggesting the dose-limiting side effects of 2-DG in CMT-7364 cells. Therefore, we explored whether the addition of HCQ can reduce the effective drug dose of 2-DG in CMT-7364 and 4T1 cells. Compared to the NC group, the viability of CMT-7364 and 4T1 cells at 48 and 72 h following treatment with HCQ and 2-DG was significantly inhibited, and their combination treatment resulted in lower cell viability and cell density than 2-DG alone (Fig. 2A). This phenomenon suggests massive cell death occurred.

A wound-healing assay was used to investigate the relationship between the decrease in cell viability and the inhibition of cell migration. We did not observe the effect of HCQ alone, whereas 2-DG and their combination significantly inhibited cell migration in CMT-7364 cells. In contrast, HCQ and 2-DG alone similarly reduced cell migration compared with the control, and their combination significantly inhibited cell migration in 4T1 cells (Fig. 2B, C). These results indicate that the combination of HCQ and 2-DG strongly suppressed cell migration effects.

Apoptosis is an essential regulatory process that maintains the cellular homeostasis of cancer cells. Therefore, the apoptotic rates were measured by Annexin V/PI staining. The results indicated that the apoptosis of the HCQ and 2-DG cotreatment group was significantly higher than that of the negative control and individual treatment groups (Fig. 2D, E). In addition, we also evaluated the protein levels of Bax, Bcl-2, C-Caspase-3 and C-PARP, which are typical apoptotic proteins in cancer cells (Fig. 2F, G). The expression levels of C-Caspase-3 proteins were detected by immunohistochemical analysis (Fig. 2H). These results are consistent with the above conclusions. Altogether, these results suggest that the combination of 2-DG and HCQ contributes to effective antitumour properties in vitro.

HCQ and 2-DG suppressed 4T1 xenograft tumour growth in vivo

To further validate the results of the in vitro experiments, a subcutaneous homotransplant mouse model was established. As the results show (Fig. 3A–C), the tumour volumes and weights of the combined treatment of HCQ and 2-DG were significantly lower than those of the negative control after 4 weeks of treatment. The results of 2-DG and 1/2 2-DG combined with HCQ treatment showed similar curves. No significant difference in body weight was encountered by the treated mice compared with the controls (Fig. 3D). We further examined the histopathological



features of tumours and vital organs by H&E staining (Fig. 3E). No evident histopathological abnormalities were observed in the spleen, heart or kidney, showing little-to-no toxic and side effects of the drugs on mice. Tumour sections of the combination group showed increased proportion of cells with fragmented nuclei

than those of 2-DG group, HCQ group and NC group, illustrating severer pathological changes of the tumour in situ treated with 2-DG and HCQ. In addition, the degree of nuclear fragmentation in tumour cells was similar in 100 mg/kg 2-DG group and 50 mg/kg 2-DG combined with HCQ group, suggesting

Fig. 2 **HCQ synergizes with 2-DG to decrease cell proliferation and promote apoptosis in 4T1 and CMT-7364 cells.** **A** Cell Counting Kit-8 kits were used to assess the proliferation of 4T1 and CMT-7364 cells treated with HCQ, 2-DG or HCQ combined with 2-DG at 0, 12, 24, 48 and 72 h. $n = 3$ independent experiments performed in quintuplicate for each condition. **B, C** Wound-healing assays of 4T1 and CMT-7364 cells after HCQ and 2-DG treatment alone or in combination for 24 h. Representative images depicting the beginning ($t = 0$ h) and the end ($t = 24$ h) of the recording period are shown. $n = 3$ independent experiments performed in triplicate for each condition. **D, E** Cell apoptosis assays of 4T1 and CMT-7364 cells treated with HCQ, 2-DG or their combination using FACS. Cells were collected and labelled with Annexin V-FITC and PI. $n = 3$ independent experiments performed in triplicate for each condition. **F, G** Western blot analyses of Bax, Bcl-2, cleaved caspase-3 (C-Casp3), and cleaved PARP (C-PARP) in cells treated with HCQ and 2-DG alone or in combination for 24 h. β -actin was used as an internal control. **H** Immunofluorescence staining of C-Casp3 in 4T1 and CMT-7364 cells, which were treated with HCQ and 2-DG alone or in combination for 24 h. Scale bar: 200 μ m. $n = 3$ independent experiments performed in triplicate for each condition. All results from three independent experiments are expressed as the mean \pm SD. * $p < 0.05$, ** $p < 0.01$, *** $p < 0.001$, **** $p < 0.0001$, ns = not significant ($p \geq 0.05$).

the dose reduction of 2-DG by the addition of HCQ. These tumour section changes were consistent with the changes of tumour volume and weight in Fig. 3A–C.

Moreover, significant tumour metastasis was observed in the liver and lung of the PBS injection control group (the metastasis was indicated by the blue line boxes in the liver section and by the cells filled between the alveoli in the lung section). Compared with the tumour metastasis in the single-drug group and the NC group, the metastatic foci in the liver and lung were significantly reduced in 2-DG and HCQ group, suggesting that the combination of drugs might reduce the tumour metastasis. However, this result needs to be supported by more experimental data, which may be the emphasis of follow-up research on the combination of 2-DG and HCQ.

Furthermore, immunofluorescence staining of the tumour sections showed that the accumulation of LC3 and Cleaved-Caspase-3 obviously increased in the 2-DG and HCQ combination treatment group, compared with NC group, HCQ group and 2-DG group (Figure S2). Therefore, it was suggested that the combination of HCQ and 2-DG could enhance the autophagy and apoptosis in 4T1 cells. Moreover, the fluorescence intensities of LC3 and Cleaved-Caspase-3 in cells treated with 50 mg/kg 2-DG combined with HCQ were similar to those in cells treated with only 100 mg/kg 2-DG, revealing that the addition of HCQ could reduce the effective concentration of 2-DG (Figure S2). Together, these observations supported that HCQ and 2-DG combination treatment exhibits stronger anticancer activity in vivo.

The HCQ and 2-DG combination treatment induces ERS via the PERK/eIF2 α /ATF-4/CHOP signalling pathway

To further investigate the enhanced anticancer effects of the combination of HCQ and 2-DG, transmission electron microscopy (TEM) was used to observe the cell morphology. Quantitative statistical analysis of the number of ER and autophagic vesicles is shown in Fig. S3. After treatment with 2-DG, the electron density, number and length of the ER in 4T1 and CMT-7364 cells increased overall. This phenomenon is in line with previous research [21]. However, after the combined treatment of HCQ and 2-DG, the length of ER of 4T1 and CMT-7364 cells was shortened to varying degrees, while the electron density and quantity barely changed (Fig. 4A). This discovery prompted us to investigate the unfolded protein response (UPR) pathways, while the PERK/eIF2 α /ATF-4/CHOP pathway is the major pathway in anaphase of ERS and can directly induce apoptosis [22, 23]. The cotreatment group dramatically induced the expression of Grp78, p-PERK, p-eIF-2 α , ATF-4 and CHOP compared with the NC group and the treatment group alone (Fig. 4B). Overall, the HCQ and 2-DG combination induces ERS by activating the PERK/eIF2 α /ATF-4/CHOP pathway in 4T1 cells and CMT-7364 cells.

Combination treatment with HCQ and 2-DG induces autophagy, the accumulation of which occurs through blockade of autophagic flux with HCQ

HCQ can increase the pH of lysosomes, which leads to inhibition of the fusion of lysosomes and autophagosomes and blocks

autophagic flux [24, 25]. As the TEM analysis showed (Fig. 4A), the combination therapy significantly promoted an increase in autophagic vacuoles. Then, Western blot analysis was utilized to detect the expression of the autophagic markers Beclin-1, LC3B-I/II in 4T1 and CMT-7364 cells. As shown in the quantified results (Fig. 5A, B), the cotreatment group dramatically increased Beclin-1 levels and LC3B lipidation, while the images of fluorescent LC3B puncta also confirmed this result (Fig. 5C, D).

DISCUSSION

Triple-negative breast tumour (TNBC) is a collective term for breast tumour subtypes that lack the oestrogen receptor and progesterone receptor and do not overexpress human epidermal growth factor receptor 2 [26]. Compared with tumours that positively express oestrogen receptor, progesterone receptor, and human epidermal growth factor receptor 2, TNBC is more aggressive and has worse treatment effects and prognosis [27]. CMT-7364 (canine origin) is a type of TNBC cell with similar invasive and transfer characteristics to MDA-MB-231 cells (human origin) [28]. For better comparison, we also studied 4T1 cells (mouse origin), which also have the semblable characteristics of TNBC [29].

2-DG, a glycolysis inhibitor, has been demonstrated to induce apoptosis in cancer cells by inhibiting glycolysis and energy production and activating the ERS pathway [13, 30, 31]. However, only the high-dose treatment of 2-DG can achieve good results for practical applications, which restricts the generalization of 2-DG to a certain extent. HCQ can cause an elevation of pH in lysosomes, which can inhibit the fusion of autophagosomes and autolysosomes and the degradation of cargo in autophagosomes [32]. Here, we show that the combined treatment of 2-DG and HCQ leads to an increase in cell apoptosis by inducing ERS and inhibiting autophagy (Fig. 6).

The transcription Factor C/EBP homologous protein (CHOP) is involved in ERS, which can regulate apoptosis through the BCL-2 protein family [33]. Under persistent ERS, CHOP can inhibit the expression of Bcl-2, Bcl-XL and Mcl-1, activate the expression of BIM and induce an increase in BAX and BAK [34]. This regulation initiates the activation of caspase-3 and PARP and leads to apoptosis [35]. In our research, we found that HCQ and 2-DG both inhibited the activity of CMT-7364 and 4T1 cells in a gradient concentration-dependent and time-dependent manner, and the combined use of HCQ and 2-DG further enhanced the inhibitory effect (Fig. 1). Similar outcomes were observed in the rate of migration and apoptosis in TNBC cells. The detection of apoptotic proteins also illustrates this point (Fig. 2). In orthotopic transplantation tumour mouse models, the therapeutic effect of 100 mg/kg 2-DG used alone was similar to that of 50 mg/kg 2-DG combined with HCQ group, both of which reduced tumour volume and weight to a certain extent (Fig. 3, Figure S2). Furthermore, the 2-DG combined with HCQ group presented a more significant therapeutic effect than the other groups (Figs. 3, S2). These results together illustrated that cotreatment with 2-DG and HCQ could effectively promote apoptosis by inhibiting autophagy to inhibit the tumour growth.

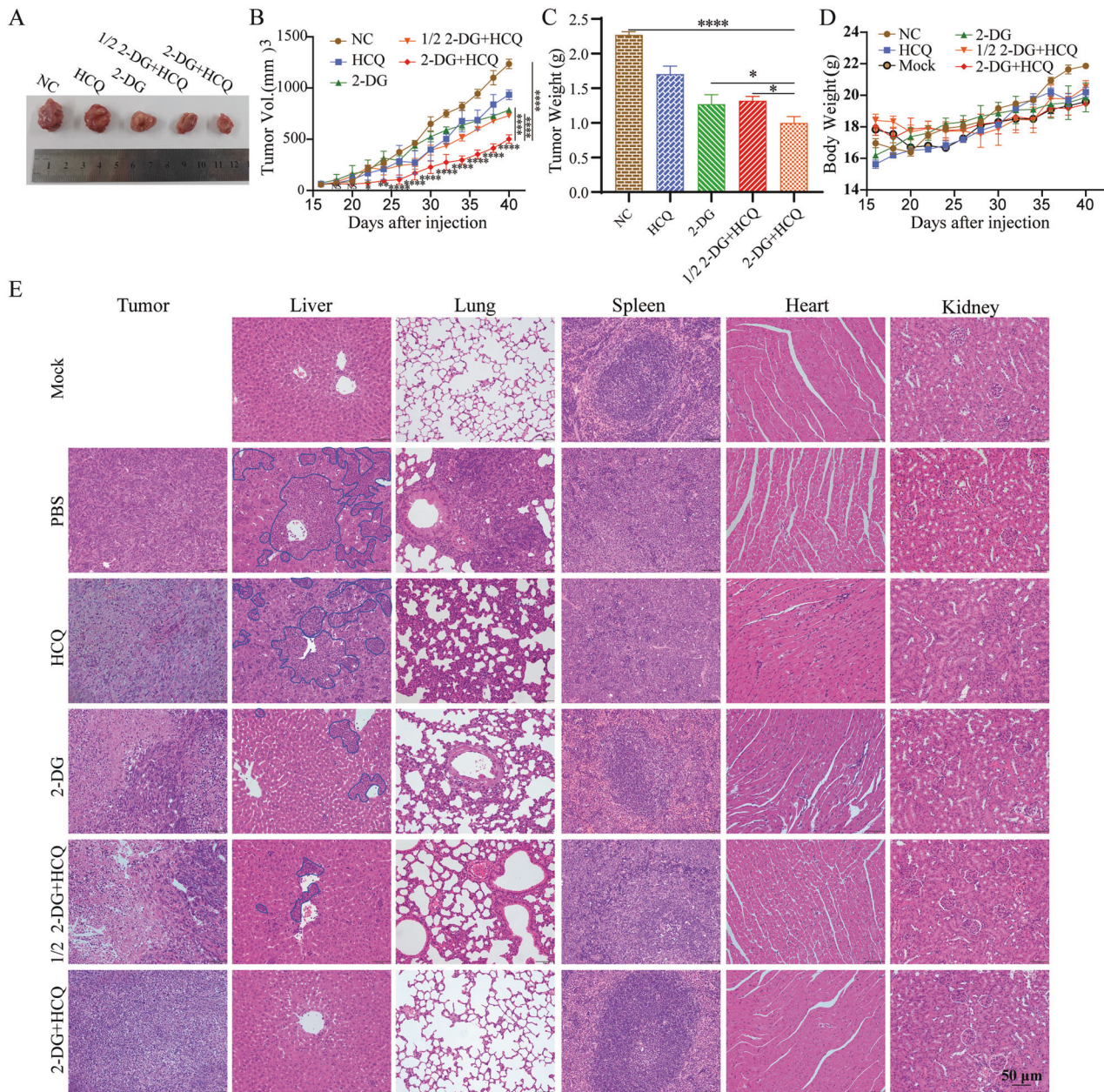


Fig. 3 **In vivo, HCQ combined with 2-DG inhibits xenograft tumour growth.** BALB/c female mice were divided into five groups, and injection of the indicated drugs began on the fifteenth. **A–C** Every 2 days, the tumour volume and body weight were measured ($n = 5$ per group). **D** On Day 40, the mice were humanely killed, samples were collected, and the tumour weight was measured. Data are shown as the mean \pm SD. The symbols ns, *, **, **** denote significant differences of not significant ($p \geq 0.05$), $P < 0.05$, $P < 0.01$, $P < 0.0001$ versus the negative control group, respectively. **E** Representative panels of H&E staining of tumours and major vital organs, such as the liver, lung, spleen, heart and kidneys of mice. Scale bar: 50 μ m. Blue-lined bordered boxes at the sections of the liver indicate metastatic 4T1 cells.

The ER is the most important organelle in the secretory function of eukaryotic cells and is responsible for the storage of calcium ions, the metabolism of lipids and carbohydrates, and the folding of proteins. Due to the special growth characteristics and environment of tumour cells, many stimulating factors, including hypoxia, lack of amino acids, and insufficient glucose supply, will affect protein processing in the ER. ERS refers to an increase in unfolded or misfolded proteins caused in the ER. To maintain cell homeostasis, cells initiate multiple basic pathways, including the UPR, endoplasmic reticulum-related degradation, autophagy, etc. Whether these regulatory programmes are sufficient to maintain cell function determines whether the cell is to restore a steady state or activate the cell death programme [36–39]. The UPR

signalling pathway consists of three major branches: protein kinase R-like ER kinase (PERK), inositol requiring enzyme 1 (IRE1) and activating transcription factor 6 (ATF6). Studies have pointed out that at the beginning of the UPR response, all branches are rapidly activated for cytoprotection. As the ERS continues, the IRE1 and ATF6 signals will be downregulated, creating an imbalance, while the PERK signal will continue to output and guide the cell towards its demise [40, 41]. Therefore, the PERK pathway was the focus of this study, as with other studies [42, 43]. The microscopic characterization of organelles was observed by TEM. The statistical analysis results of TEM are shown in Fig. S3. We found that the number of widened ERs was significantly increased in TNBC cells treated with HCQ. However, after 2-DG

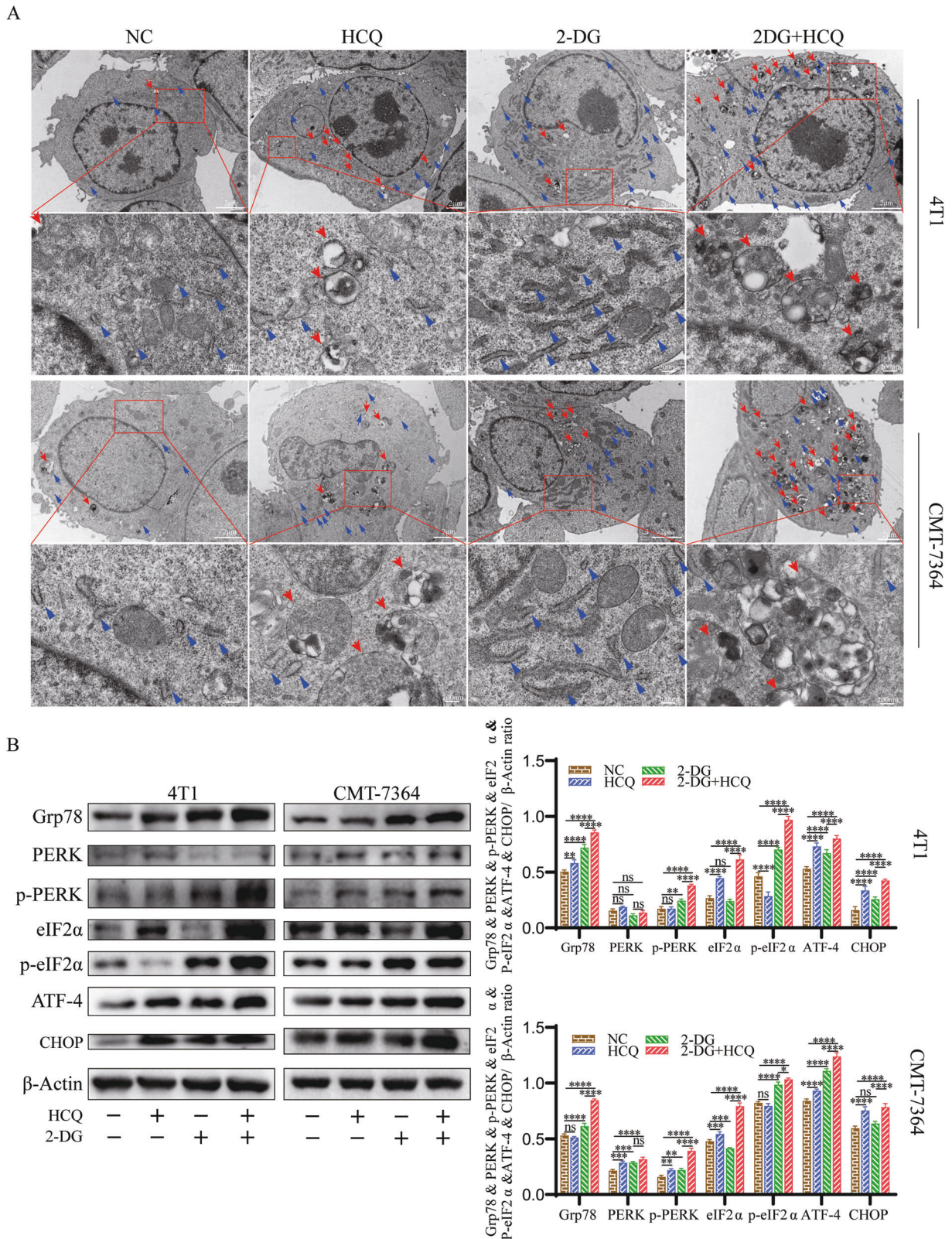


Fig. 4 HCQ and 2-DG synergistically promote endoplasmic reticulum stress through the PERK/eIF2 α /ATF-4 pathway. **A** Representative TEM images depicting the ultrastructure of 4T1 and CMT-7364 cells treated without or with HCQ, 2-DG or 2-DG combined with HCQ for 24 h. Red arrows indicate autophagic vacuoles; blue arrows indicate endoplasmic reticulum. Scale bars: 2 mm (Thumbnail), 200 nm (Enlarge image). **B** Western blot analyses of Grp78, PERK, p-PERK, eIF2 α , p-eIF2 α , ATF-4 and CHOP in cells treated with HCQ and 2-DG alone or in combination for 24 h. β -actin was used as an internal control. Data are represented as mean \pm SD from three independent experiments. * p < 0.05, ** p < 0.01, *** p < 0.001, **** p < 0.0001, ns = not significant ($p \geq 0.05$).

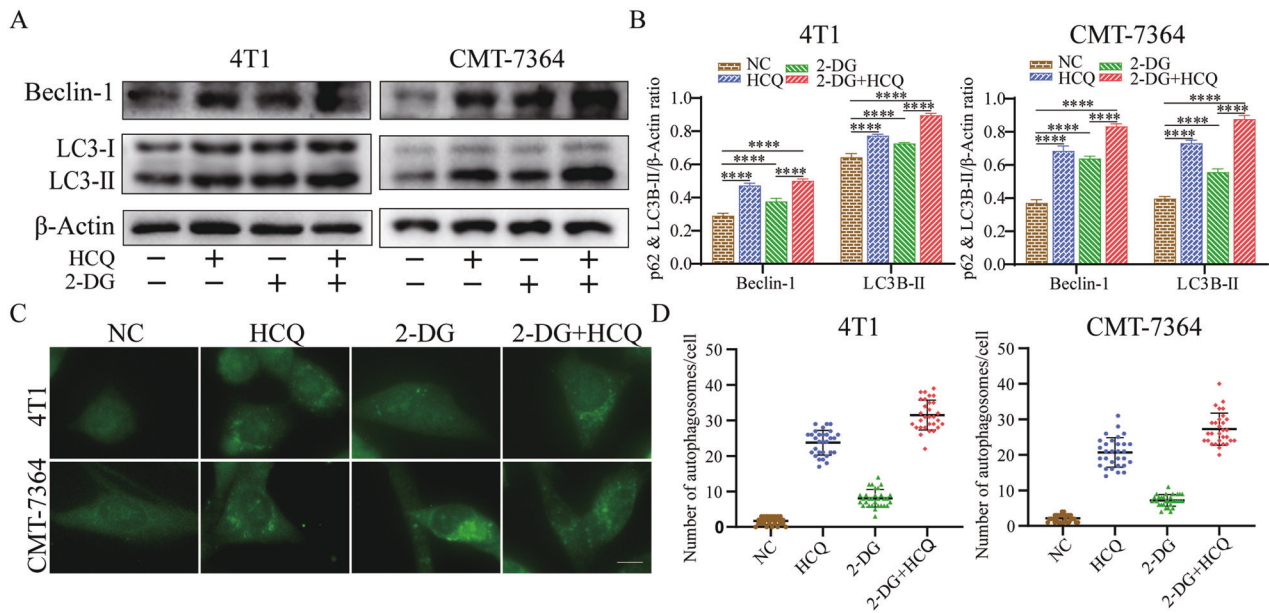


Fig. 5 HCQ combined with 2-DG inhibits autophagic degradation in 4T1 cells and CMT-7364 cells. **A, B** Western blot analyses of Beclin-1 and LC3B-II in 4T1 and CMT-7364 cells that were treated without or with HCQ, 2-DG or 2-DG combined with HCQ for 24 h. β -actin was used as an internal control. Data are represented as mean \pm SD from three independent experiments. $^{**}p < 0.01$, $^{****}p < 0.0001$. **C, D** Immunofluorescence staining of LC3B-II in 4T1 and CMT-7364 cells, which were treated with HCQ and 2-DG alone or in combination for 24 h. Scale bar: 10 μ m. $n = 3$ independent experiments performed in triplicate for each condition and at least 30 cells scored.

treatment, the number, electron density and length of ER in cells all increased significantly compared with NC. Interestingly, ER was significantly shorter in the cotreatment group, but its number and electron density remained at a high level. We hypothesized that the ER, as the main source of the intracellular plasma membrane, provides membrane sources for the massively formed autophagic vesicles, thereby shortening the length of its own plasma membrane [44, 45]. WB results showed that HCQ combined with 2-DG significantly increased ERS levels through the PERK-eIF2 α -ATF-4-CHOP pathway (Fig. 4).

From yeast to mammals, autophagy is an evolutionarily conserved process [46, 47]. A high degree of autophagy has been found in many tumour cells to maintain cell survival [48, 49]. Autophagy participates in the degradation of damaged proteins/organelles in cells and converts them into amino acids [50]. These findings support the importance of autophagy in sustaining cellular homeostasis. TEM showed an increase in autophagic vesicles in TNBC cells after 2-DG treatment compared with NC. Previous studies have shown that 2-DG induces the formation of autophagosomes to enhance autophagy [51]. Combined with our study, it is speculated that 2-DG might induce protective autophagy response by glucose deprivation [52–55]. Therefore, blocking protective autophagy has become the subject of many studies [56–58]. HCQ was applied to block the protective autophagy in our study. In TNBC cells treated with a combination of 2-DG and HCQ, the number of autophagic vesicles and the protein levels of Beclin-1 and LC3B-II increased significantly than those treated with the single-drug groups (Figs. 4 and 5). It is indicated that HCQ terminated the protective autophagy induced by 2-DG.

In this study, we demonstrated the effective antitumoral effect of the combination of 2-DG and HCQ on TNBC cells both in vivo and in vitro. Indeed, the remarkable efficiency of their combination to affect cell viability by autophagy inhibition and continuous ERS may have important implications in the treatment of breast cancer.

MATERIALS AND METHODS

Cell culture

The 4T1 cells used in this study were obtained from the Chinese Academy of Sciences Cell Bank (Shanghai, China), and CMT-7364 cells, a cell line isolated from canine breast tumour, were kindly provided by the Degui Lin Laboratory at the China Agricultural University [59]. All cell lines were grown in RPMI 1640 medium with 10% foetal bovine serum and 1% penicillin–streptomycin at 37 °C with 5% CO₂. Cells were cultured in T25 cell culture flasks. When the cell density reached more than 80%, the cells were subcultured into 96-well plates or 6-well plates for the corresponding experiments.

Reagents and antibodies

Western blotting and immunofluorescence were performed using the following antibodies: phospho-PERK (p-PERK), phospho-eIF2 α (p-eIF2 α), cleaved-Caspase-3 (c-Casp3), β -actin (Cell Signalling Technologies; Danvers, MA); cleaved-PARP (c-PARP), CHOP, Bax, Bcl-2, Grp78, PERK, eIF2 α , ATF-4, Beclin-1, LC3B-I/II (Abcam, Cambridge, UK). 2-DG (purity $\geq 98\%$) and HCQ (purity $>99\%$) were obtained from Sigma-Aldrich Chemical (Agent of Shanghai, China). The Apoptosis Assay Kit and FITC Annexin V Apoptosis Detection Kit with PI (propidium iodide) were purchased from the Beyotime Institute of Biotechnology (Shanghai, China). The Cell Counting Kit-8 was purchased for cell viability detection (CCK-8, Dojindo Laboratories, Minato-ku, Tokyo, Japan). All of the other chemicals and reagents were of the highest commercial grade availability.

Cell viability (CCK-8) assay

Cells were seeded in 96-well plates at a density of 2×10^4 cells/mL (37 °C, 12 h). There were five repeats for one group, and different concentrations of 2-DG (0.25, 0.5, 1, 2 or 4 mM) combined with or without HCQ (10 μ M) and HCQ (5, 10, 20, 40, 80, 120, 160, 200 or 400 μ M) were added and incubated for another 24 h. In the other set of experiments, cells were cultured with PBS, HCQ (10 μ M), 2-DG (1 mM), or 2-DG (1 mM) combined with HCQ (10 μ M) for different times (12, 24, 48 or 72 h). Culture medium with the same concentration of drugs was changed every 12 h unless otherwise indicated. After treatment, a total of 10 μ L (5 mg/mL) of CCK-8 was added per well and incubated at 37 °C for 1 h. Cell viability was measured through absorbance (optical density) with a microplate reader (Bio-Rad Instruments, Hercules, CA) at 450 nm.

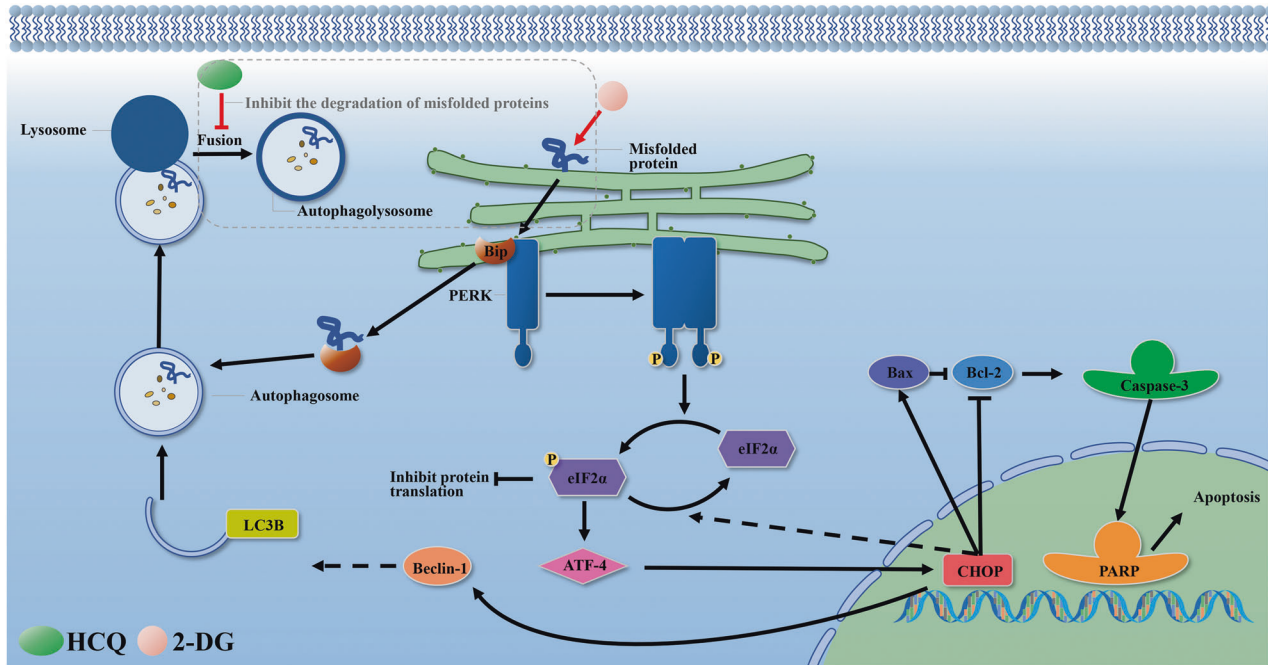


Fig. 6 Schematic illustration delineating the role of HCQ/2-DG combination therapy. The metabolites of 2-DG interfere with the N-linked glycosylation of proteins, leading to the accumulation of unfolded/misfolded proteins in the ER, followed by ERS, apoptosis, and cytoprotective autophagy. HCQ causes deacidification of lysosomes, inhibits the fusion of autophagosomes and lysosomes to form autophagolysosomes, which results in the inhibition of misfolded protein degradation and further induces endoplasmic reticulum stress, ultimately leading to increased apoptosis.

Wound-healing migration assay

Cell migration was assessed by wound-healing scratch assays as previously described. CMT-7364 cells and 4T1 cells were seeded into 6-well tissue culture plates. When cells grew to 80% confluence, scratches were made using 200 μ L plastic pipette tips, and the cells were washed twice with PBS carefully. Then, the cells were stimulated with Opti-MEM (Invitrogen, CA) reduced serum medium containing PBS, HCQ, 2-DG or 2-DG combined with HCQ for 24 h. Images were taken from an inverted microscope connected to a Canon camera. ImageJ software was used to measure the gap distance of the wound.

Apoptosis assay

Apoptosis assays were performed using Annexin V-FITC (fluorescein isothiocyanate) and propidium iodide (PI) double staining. CMT-7364 cells and 4T1 cells were cultured in 6-well plates for 12 h. After the predetermined treatment was reached, the cells were washed twice with precooled PBS. The cells were digested with trypsin and centrifuged at a speed of 1000 rpm/min for 5 min, washed twice with precooled PBS, and resuspended in binding buffer (500 μ L) at a concentration of 1×10^6 cells/mL. The cells were gently vortexed and incubated with 5 μ L of Annexin V-FITC and 10 μ L of propidium iodide at room temperature for 10 min in the dark per the manufacturer's instructions. The apoptosis rates were determined by flow cytometry (Becton Dickinson; Franklin Lakes, New Jersey) and analysed by FlowJo 10.6.2 software.

Transmission electron microscopy

CMT-7364 cells and 4T1 cells were cultured in 6-well plates. After treatment, cells were fixed (4 $^{\circ}$ C, overnight) using 2.0% (v/v) paraformaldehyde and 2.5% (v/v) glutaraldehyde in 0.1 M PBS. Cells were washed in PBS, fixed in 1% osmium tetroxide at room temperature (20 $^{\circ}$ C) for 2 h, and then washed three times in PBS. After that, the cells were dehydrated in a graded acetone series (30%, 50%, 70%, 80%, 85%, 90%, 95%, 100% (v/v) ethanol). The last step was repeated twice for 20 min each time. The specimens were permeabilized at a 2:1 mixture of acetone and Epon overnight at 37 $^{\circ}$ C, then placed in acetone in Epon (1:1 mixture) for 8 h at 37 $^{\circ}$ C and finally in pure Epon overnight at 37 $^{\circ}$ C. Then, the cells were transferred to a casting mould for polymerization at 60 $^{\circ}$ C. The specimens were sectioned to a thickness of 80 μ m (Leica, Wetzlar, Germany). The sections were placed in a mesh copper grid and stained with 2% uranium acetate and lead citrate. Then, the

sections were dried overnight at room temperature and examined using a transmission electron microscope (Hitachi, Tokyo, Japan).

Western blotting

Western blot (WB) analysis was carried out according to previous methods and briefly described as follows. The total protein of cells was harvested with a RIPA lysis solution involving PMSF and phosphatase inhibitors (BioSharp, Hefei, China). Sample proteins were separated by SDS-PAGE and transferred to PVDF membranes. The membrane was blocked for 2 h in 5% skim milk, followed by treatment with primary antibody and secondary antibody. Proteins were visualized with a ChemiDoc MP imaging system (Bio-Rad, USA), and protein expression was analysed with ImageJ software.

Immunofluorescence staining

Immunofluorescence (IF) staining was carried out according to previous methods and briefly described as follows. CMT-7364 cells and 4T1 cells were cultured in 24-well plates at a density of 1×10^5 cells/mL. After treatment, cells were fixed with 4% (v/v) paraformaldehyde for 30 min and permeabilized with 0.5% Triton X-100 in PBS for 20 min. Subsequently, the cells were blocked with 5% BSA for 2 h and incubated with primary antibodies overnight at 4 $^{\circ}$ C. FITC-labelled or Cy3-labelled goat anti-rabbit IgG (H + L) was used to incubate the cells in the dark for 1 h and stain with 4,6-diamidino-2-phenylindole (DAPI, Beyotime, China) for nuclear counterstaining for 2 min. In this experiment, the cells were washed three times with PBS between each treatment. Images were observed under a fluorescence microscope (Olympus, Tokyo, Japan).

In vivo experiments

Six-week-old BALB/c (16–18 g) female mice were purchased from the Hubei Province Experimental Animal Center of Huazhong Agricultural University (Wuhan, China) a week prior to the experiments. The experimental animals were cared for and used under the guidelines of the Institutional Ethical Committee for Animal Care and Use of Huazhong Agricultural University and United States National Institutes of Health. Approximately 5×10^7 4T1 cells were collected and suspended in 2.5 mL of PBS and then subcutaneously injected into the fourth breast pad of the mice. The mice developed obvious lumps two weeks after the injection. These mice were

randomized into five groups and all intraperitoneally injected with different drugs. The mice in the first group were treated with HCQ (50 mg/kg, every other day for 25 days). The mice in the second group were treated with 2-DG (100 mg/kg, every other day for 25 days). The mice in the third group were treated with 1/2 2-DG (50 mg/kg, every other day for 25 days) and HCQ (50 mg/kg, every other day for 25 days) at the same time. The mice in the fourth group were treated with 2-DG (100 mg/kg, every other day for 25 days) and HCQ (50 mg/kg, every other day for 25 days) at the same time. The last group was treated with PBS as the control group. Tumour volume and body weight were measured every 2 days. Tumour volume ($V = 0.5 \times \text{length} \times \text{width}^2$). Finally, mice were humanely killed at the end of the experiment, tumours were harvested and weighed, and major vital organs, such as the liver, lung, spleen, heart and kidney, from each group were harvested and fixed in 4% paraformaldehyde.

Mouse tissue section staining

Tumours and organs were subsequently dehydrated and embedded in paraffin 48 h after fixation in formaldehyde and later cut into 5- μm -thick slices for haematoxylin and eosin (H&E) staining. An optical microscope (Olympus, Japan) was used for image collection. The tumour sections were also applied for immunofluorescence staining.

The tumour sections were also applied for immunofluorescence staining. After dewaxed by xylene and gradient ethanol to water, the tumour sections were immersed in citric acid antigen repair buffer (pH 6.0) and heated in a microwave oven for antigen repair. Then, tumour sections were subjected to a similar procedure to step 2.8, including blocking with goat serum, incubating with primary and secondary antibodies, counterstaining with DAPI, and sealed with anti-fluorescence quenching sealing tablets. Images were observed under a fluorescence microscope (Olympus, Tokyo, Japan).

Statistical analysis

Data are presented as the means \pm standard deviation (means \pm SD) of at least three independent experiments. The intergroup differences were calculated by two-way analysis of variance or unpaired Student's *t* test (GraphPad Prism 8). A level of $*p < 0.05$ was considered significant, and $**p < 0.01$, $***p < 0.001$, or $****p < 0.0001$ was considered extremely significant. A level of $p > 0.05$ (ns) was considered not significant.

DATA AVAILABILITY

All data are available in the main text or in the supplementary materials.

REFERENCES

- Grabinski VF, Brawley OW. Disparities in breast cancer. *Obstet Gynecol Clin North Am.* 2022;49:149–65.
- Torre LA, Islami F, Siegel RL, Ward EM, Jemal A. Global cancer in women: burden and trends. *Cancer Epidemiol Biomark Prev.* 2017;26:444–57.
- Garden OA, Volk SW, Mason NJ, Perry JA. Companion animals in comparative oncology: one Medicine in action. *Vet J.* 2018;240:6–13.
- Kaszak I, Ruszczak A, Kanafa S, Kacprzak K, Król M, Jurka P. Current biomarkers of canine mammary tumors. *Acta Vet Scand.* 2018;60:66.
- Curigliano G, Cardinale D, Dent S, Criscitiello C, Aseyev O, Lenihan D, et al. Cardiotoxicity of anticancer treatments: epidemiology, detection, and management. *CA Cancer J Clin.* 2016;66:309–25.
- Brown JM, Attardi LD. The role of apoptosis in cancer development and treatment response. *Nat Rev Cancer.* 2005;5:231–7.
- Warburg O. Über den stoffwechsel der carcinomzelle. *Naturwissenschaften* 1924;12:1131–7.
- Choe M, Brusgard JL, Chumsri S, Bhandary L, Zhao XF, Lu S, et al. The RUNX2 transcription factor negatively regulates SIRT6 expression to alter glucose metabolism in breast cancer Cells. *J Cell Biochem.* 2015;116:2210–26.
- Ralsler M, Wamelink MM, Struys EA, Joppich C, Krobtsch S, Jakobs C, et al. A catabolic block does not sufficiently explain how 2-deoxy-D-glucose inhibits cell growth. *Proc Natl Acad Sci USA.* 2008;105:17807–11.
- Zhang D, Li J, Wang F, Hu J, Wang S, Sun Y. 2-Deoxy-D-glucose targeting of glucose metabolism in cancer cells as a potential therapy. *Cancer Lett.* 2014;355:176–83.
- Kurtoglu M, Gao N, Shang J, Maher JC, Lehrman MA, Wangpaichit M, et al. Under normoxia, 2-deoxy-D-glucose elicits cell death in select tumor types not by inhibition of glycolysis but by interfering with N-linked glycosylation. *Mol Cancer Ther.* 2007;6:3049–58.
- Saito S, Furuno A, Sakurai J, Sakamoto A, Park H-R, Shin-Ya K, et al. Chemical genomics identifies the unfolded protein response as a target for selective cancer cell killing during glucose deprivation. *Cancer Res.* 2009;69:4225–34.
- Ahadova A, Gebert J, von Knebel Doeberitz M, Kopitz J, Kloor M. Dose-dependent effect of 2-deoxy-D-glucose on glycoprotein mannosylation in cancer cells. *IUBMB Life.* 2015;67:218–26.
- Maschek G, Savaraj N, Priebe W, Braunschweiger P, Hamilton K, Tidmarsh GF, et al. 2-deoxy-D-glucose increases the efficacy of adriamycin and paclitaxel in human osteosarcoma and non-small cell lung cancers in vivo. *Cancer Res.* 2004;64:31–34.
- Wu H, Zhu H, Liu DX, Niu T-K, Ren X, Patel R, et al. Silencing of elongation factor-2 kinase potentiates the effect of 2-deoxy-D-glucose against human glioma cells through blunting of autophagy. *Cancer Res.* 2009;69:2453–60.
- Costedoat-Chalumeau N, Amoura Z, Hulot J-S, Lechat P, Piette J-C. Hydroxychloroquine in systemic lupus erythematosus. *Lancet* 2007;369:1257–8.
- Yao X, Ye F, Zhang M, Cui C, Huang B, Niu P, et al. In vitro antiviral activity and projection of optimized dosing design of hydroxychloroquine for the treatment of severe acute respiratory syndrome coronavirus 2 (SARS-CoV-2). *Clin Infect Dis.* 2020;71:732–9.
- Du W, Xu A, Huang Y, Cao J, Zhu H, Yang B, et al. The role of autophagy in targeted therapy for acute myeloid leukemia. *Autophagy* 2021;17:2665–79.
- Chen M-Y, Yadav VK, Chu YC, Ong JR, Huang T-Y, Lee K-F, et al. Hydroxychloroquine (HCQ) modulates autophagy and oxidative DNA damage stress in hepatocellular carcinoma to overcome sorafenib resistance via TLR9/SOD1/hsa-miR-30a-5p/Beclin-1 axis. *Cancers.* 2021;13:3227.
- Dai S, Peng Y, Zhu Y, Xu D, Zhu F, Xu W, et al. Glycolysis promotes the progression of pancreatic cancer and reduces cancer cell sensitivity to gemcitabine. *Biomed Pharmacother.* 2020;121:109521.
- Giammarioli AM, Gambardella L, Barbati C, Pietraforte D, Tinari A, Alberton M, et al. Differential effects of the glycolysis inhibitor 2-deoxy-D-glucose on the activity of pro-apoptotic agents in metastatic melanoma cells, and induction of a cytoprotective autophagic response. *Int J Cancer.* 2012;131:E337–347.
- Liu J, Han P, Li M, Yan W, Liu J, He J, et al. Histidine-rich calcium binding protein promotes growth of hepatocellular carcinoma in vitro and in vivo. *Cancer Sci.* 2015;106:1288–95.
- Shin S, Buel GR, Wolgamott L, Plas DR, Asara JM, Blenis J, et al. ERK2 mediates metabolic stress response to regulate cell Fate. *Mol Cell.* 2015;59:382–98.
- Soto-Pantoja DR, Miller TW, Pendrak ML, DeGraff WG, Sullivan C, Ridnour LA, et al. CD47 deficiency confers cell and tissue radioprotection by activation of autophagy. *Autophagy* 2012;8:1628–42.
- Lao Y, Wan G, Liu Z, Wang X, Ruan P, Xu W, et al. The natural compound oblongifolin C inhibits autophagic flux and enhances antitumor efficacy of nutrient deprivation. *Autophagy* 2014;10:736–49.
- Boyle P. Triple-negative breast cancer: epidemiological considerations and recommendations. *Ann Oncol.* 2012;23:vi7–v12. Suppl 6
- Garrido-Castro AC, Lin NU, Polyak K. Insights into molecular classifications of triple-negative breast cancer: improving patient selection for treatment. *Cancer Disco.* 2019;9:176–98.
- Zhang H, Pei S, Zhou B, Wang H, Du H, Zhang D, et al. Establishment and characterization of a new triple-negative canine mammary cancer cell line. *Tissue Cell.* 2018;54:10–19.
- Schrörs B, Boegel S, Albrecht C, Bukur T, Bukur V, Holtsträter C, et al. Multi-omics characterization of the 4T1 murine mammary gland tumor model. *Front Oncol.* 2020;10:1195.
- Yu S-M, Kim S-J. Endoplasmic reticulum stress (ER-stress) by 2-deoxy-D-glucose (2DG) reduces cyclooxygenase-2 (COX-2) expression and N-glycosylation and induces a loss of COX-2 activity via a Src kinase-dependent pathway in rabbit articular chondrocytes. *Exp Mol Med.* 2010;42:777–86.
- Liu H, Kurtoglu M, Cao Y, Xi H, Kumar R, Axten JM, et al. Conversion of 2-deoxyglucose-induced growth inhibition to cell death in normoxic tumor cells. *Cancer Chemother Pharm.* 2013;72:251–62.
- Klionsky DJ, Abeliovich H, Agostinis P, Agrawal DK, Aliev G, Askew DS, et al. Guidelines for the use and interpretation of assays for monitoring autophagy in higher eukaryotes. *Autophagy* 2008;4:151–75.
- Zagorodna O, Martin SM, Rutkowski DT, Kuwana T, Spitz DR, Knudson CM. 2-deoxyglucose-induced toxicity is regulated by Bcl-2 family members and is enhanced by antagonizing Bcl-2 in lymphoma cell lines. *Oncogene* 2012;31:2738–49.
- Iurlaro R, Muñoz-Pinedo C. Cell death induced by endoplasmic reticulum stress. *FEBS J.* 2016;283:2640–52.
- Jeyaraj M, Rajesh M, Arun R, MubarakAli D, Sathishkumar G, Sivanandhan G, et al. An investigation on the cytotoxicity and caspase-mediated apoptotic effect of biologically synthesized silver nanoparticles using Podophyllum hexandrum on human cervical carcinoma cells. *Colloids Surf B, Biointerfaces.* 2013;102:708–17.
- Hetz C. The unfolded protein response: controlling cell fate decisions under ER stress and beyond. *Nat Rev Mol Cell Biol.* 2012;13:89–102.

37. Rutkowski DT, Hegde RS. Regulation of basal cellular physiology by the homeostatic unfolded protein response. *J Cell Biol.* 2010;189:783–94.
38. Walter P, Ron D. The unfolded protein response: from stress pathway to homeostatic regulation. *Science* 2011;334:1081–6.
39. Shore GC, Papa FR, Oakes SA. Signaling cell death from the endoplasmic reticulum stress response. *Curr Opin Cell Biol.* 2011;23:143–9.
40. Lin JH, Li H, Yasumura D, Cohen HR, Zhang C, Panning B, et al. IRE1 signaling affects cell fate during the unfolded protein response. *Science* 2007;318:944–9.
41. Rutkowski DT, Arnold SM, Miller CN, Wu J, Li J, Gunnison KM, et al. Adaptation to ER stress is mediated by differential stabilities of pro-survival and pro-apoptotic mRNAs and proteins. *PLoS Biol.* 2006;4:e374.
42. Xi H, Kurtoglu M, Liu H, Wangpaichitr M, You M, Liu X, et al. 2-Deoxy-D-glucose activates autophagy via endoplasmic reticulum stress rather than ATP depletion. *Cancer Chemother Pharm.* 2011;67:899–910.
43. León-Annicchiarico CL, Ramírez-Peinado S, Domínguez-Villanueva D, Gonsberg A, Lampidis TJ, Muñoz-Pinedo C. ATF4 mediates necrosis induced by glucose deprivation and apoptosis induced by 2-deoxyglucose in the same cells. *FEBS J.* 2015;282:3647–58.
44. Nelson C, Ambros V, Baehrecke EH. miR-14 regulates autophagy during developmental cell death by targeting ip3-kinase 2. *Mol Cell.* 2014;56:376–88.
45. English L, Chemali M, Duron J, Rondeau C, Laplante A, Gingras D, et al. Autophagy enhances the presentation of endogenous viral antigens on MHC class I molecules during HSV-1 infection. *Nat Immunol.* 2009;10:480–7.
46. Mizushima N, Yoshimori T, Ohsumi Y. The role of Atg proteins in autophagosome formation. *Annu Rev Cell Develop Biol.* 2011;27:107–32.
47. Levy JMM, Towers CG, Thorburn A. Targeting autophagy in cancer. *Nat Rev Cancer.* 2017;17:528–42.
48. Kaminsky VO, Piskunova T, Zborovskaya IB, Tchevkina EM, Zhivotovsky B. Suppression of basal autophagy reduces lung cancer cell proliferation and enhances caspase-dependent and -independent apoptosis by stimulating ROS formation. *Autophagy* 2012;8:1032–44.
49. Yang S, Wang X, Contino G, Liesa M, Sahin E, Ying H, et al. Pancreatic cancers require autophagy for tumor growth. *Genes Dev.* 2011;25:717–29.
50. Mathew R, Karp CM, Beaudoin B, Vuong N, Chen G, Chen HY, et al. Autophagy suppresses tumorigenesis through elimination of p62. *Cell* 2009;137:1062–75.
51. Wang Q, Liang B, Shirwany NA, Zou MH. 2-Deoxy-D-glucose treatment of endothelial cells induces autophagy by reactive oxygen species-mediated activation of the AMP-activated protein kinase. *PLoS ONE.* 2011;6:e17234.
52. Rabinowitz JD, White E. Autophagy and metabolism. *Science* 2010;330:1344–8.
53. Matsui Y, Takagi H, Qu X, Abdellatif M, Sakoda H, Asano T, et al. Distinct roles of autophagy in the heart during ischemia and reperfusion: roles of AMP-activated protein kinase and Beclin 1 in mediating autophagy. *Circulation Res.* 2007;100:914–22.
54. Lum JJ, Bauer DE, Kong M, Harris MH, Li C, Lindsten T, et al. Growth factor regulation of autophagy and cell survival in the absence of apoptosis. *Cell* 2005;120:237–48.
55. Roberts DJ, Tan-Sah VP, Ding EY, Smith JM, Miyamoto S. Hexokinase-II positively regulates glucose starvation-induced autophagy through TORC1 inhibition. *Mol Cell.* 2014;53:521–33.
56. Liu LQ, Wang SB, Shao YF, Shi JN, Wang W, Chen WY, et al. Hydroxychloroquine potentiates the anti-cancer effect of bevacizumab on glioblastoma via the inhibition of autophagy. *Biomed Pharmacother.* 2019;118:109339.
57. Ben Sahara I, Laurent K, Giuliano S, Larbret F, Ponzio G, Gounon P, et al. Targeting cancer cell metabolism: the combination of metformin and 2-deoxyglucose induces p53-dependent apoptosis in prostate cancer cells. *Cancer Res.* 2010;70:2465–75.
58. Aravindan S, Ramraj SK, Somasundaram ST, Aravindan N. Novel adjuvants from seaweed impede autophagy signaling in therapy-resistant residual pancreatic cancer. *J Biomed Sci.* 2015;22:28.
59. Zhang H, Pei S, Zhou B, Wang H, Du H, Zhang D, et al. Establishment and characterization of a new triple-negative canine mammary cancer cell line. *Tissue Cell.* 2018;54:10–19.

ACKNOWLEDGEMENTS

The authors thank Prof. Degui Lin (China Agricultural University, Beijing, China) for providing the CMT-7364 cell line.

AUTHOR CONTRIBUTIONS

Conceptualization: NZ and QL; methodology: NZ, QL and XW; project administration: NZ, QL, LH, TZ (Tao Zhang), HZ, XZ and TZ (Tianhong Zhou); writing—original draft: NZ, QL and XW; writing—review and editing: NZ, QL, GD and CQ. All authors have read and agreed to the published version of the manuscript.

FUNDING

Project supported by the National Natural Science Foundation of China (Grant No. 32172925).

COMPETING INTERESTS

The authors declare no competing interests.

ADDITIONAL INFORMATION

Supplementary information The online version contains supplementary material available at <https://doi.org/10.1038/s41420-022-01074-6>.

Correspondence and requests for materials should be addressed to Changwei Qiu.

Reprints and permission information is available at <http://www.nature.com/reprints>

Publisher's note Springer Nature remains neutral with regard to jurisdictional claims in published maps and institutional affiliations.



Open Access This article is licensed under a Creative Commons Attribution 4.0 International License, which permits use, sharing, adaptation, distribution and reproduction in any medium or format, as long as you give appropriate credit to the original author(s) and the source, provide a link to the Creative Commons license, and indicate if changes were made. The images or other third party material in this article are included in the article's Creative Commons license, unless indicated otherwise in a credit line to the material. If material is not included in the article's Creative Commons license and your intended use is not permitted by statutory regulation or exceeds the permitted use, you will need to obtain permission directly from the copyright holder. To view a copy of this license, visit <http://creativecommons.org/licenses/by/4.0/>.

© The Author(s) 2022